

ELECTRONIC SUPPLEMENTARY INFORMATION

UiO-66 framework with encapsulated spin probe: synthesis and exceptional sensitivity to mechanical pressure

Artem S. Poryvaev,^{*a} Kirill P. Larionov,^b Yana N. Albrekht,^a Alexander A. Efremov,^{a,c} Alexey S. Kiryutin,^a Kristina A. Smirnova,^{a,c} Vasilii Y. Evtushok,^b Matvey V. Fedin ^{*a}

^aInternational Tomography Center SB RAS, Novosibirsk, 630090, Russia

^bBoreskov Institute of Catalysis SB RAS, Lavrentiev av. 5, 630090 Novosibirsk, Russia

^cNovosibirsk State University, Pirogova str. 1, 630090, Novosibirsk, Russia

Table of contents:

I. Characterization of sample	S2
I.1. PXRD data	S2
I.2. Textural characteristics of UiO-66.....	S3
I.3. N ₂ adsorption measurements.....	S4
II. Supplementary data	S5
II.1 Supplementary NMR data	S5
II.1. Supplementary EPR data	S6
Kinetics of TEMPO@UiO-66 formation	S6
Methodology for characterization of the content of nitroxide probe in MOF pores	S7
Encapsulation of TEMPO in UiO-66	S8
Mechanical pressure applied to TEMPO@ZIF-8.....	S10
Different mechanical pressure applied to TEMPO@UiO-66.....	S11
II.2. Supplementary TGA data	S13
II.3. Supplementary PXRD data.....	S14
II.4. Supplementary N ₂ adsorption measurements	S15
III. References	S16

I. Characterization of sample

I.1. PXRD data

The studied sample TEMPO@UiO-66 was characterized by powder X-ray diffraction (PXRD). The PXRD pattern (Fig. S1 black) showed typical 2θ peak positions for UiO-66 (~ 8 , 9 and 25°). Also peak positions correspond well to the simulated PXRD data for UiO-66 obtained using Mercury 3.3 (Fig. S1 blue).

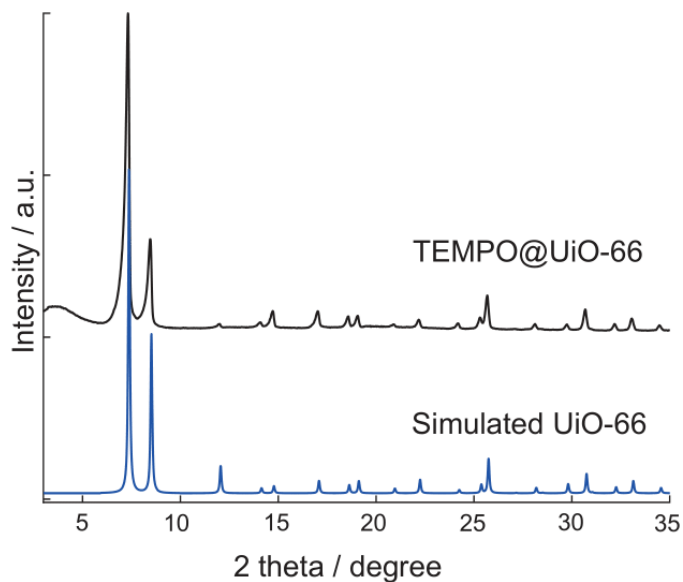


Fig. S1. PXRD data for TEMPO@UiO-66 (black) and UiO-66 simulated by Mercury 3.3 (blue).

I.2. Textural characteristics of UiO-66

Table S1. Textural characteristics of UiO-66.

Sample	S_{total} , m^2/g	V_{total} , cm^3/g	Particle size, nm
UiO-66	1113	0.53	450
TEMPO@UiO-66	1073	0.49	400

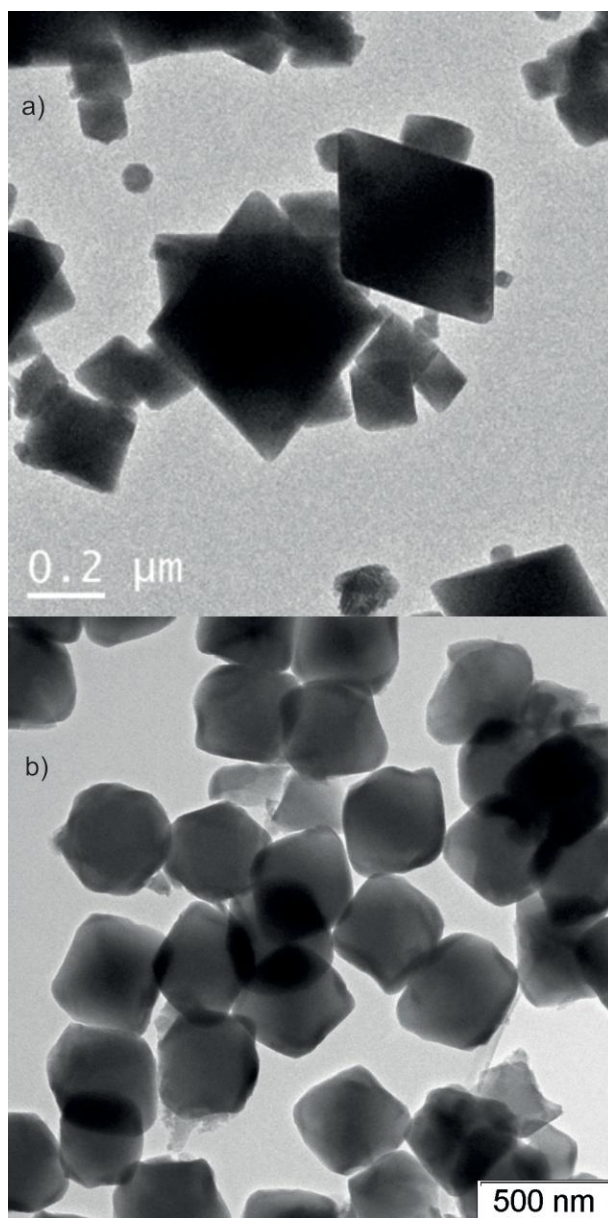


Fig. S2. HRTEM image of UiO-66 (a) and TEMPO@UiO-66 (b).

I.3. N₂ adsorption measurements

It was shown that BET surface area for the initial UiO-66 was slightly larger (1113 m²/g) than that for UiO-66 with incorporated TEMPO (1073 m²/g). Thus, nitroxide encapsulation has led to an insignificant decrease of specific surface area. Also, BET surface area for pristine MOF is consistent with values reported in the literature for this MOF.^{S1} The shape of the N₂ adsorption isotherms for both samples exhibit type I behavior (Fig. S3).

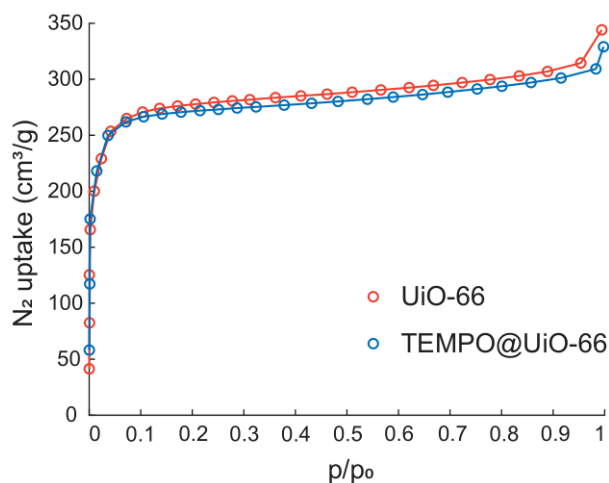


Fig. S3. N₂ adsorption isotherms for UiO-66 (red) and TEMPO@UiO-66 (blue) at 77 K.

II. Supplementary data

II.1 Supplementary NMR data

Since TEMPOH are diamagnetic molecules we have studied TEMPOH:BDC ratio in the TEMPOH@UiO-66 sample using NMR approach. For this sake we dissolved TEMPOH*HCl@UiO-66 in HF/d₆-DMSO mixture (details in Experimental part). Then we have measured ¹H NMR spectrum for the solution and analyzed ratio between TEMPOH and 1,4-benzenedicarboxylate (Fig. S4). To avoid ¹³C satellites we applied ¹³C broadband decoupling during acquisition of free induction decay. To avoid strong residual signal from water-HF protons we applied standard excitation sculpting sequence for water suppression at 6.1 ppm. We have found the following ratio TEMPOH : 1,4-benzenedicarboxylate = 1 : 694±200 (error is based on reproducibility with different samples). We thus estimated that there is 1 TEMPOH molecule per 154±50 Zr₆ clusters, taking into account that MOF structure is not ideal (TGA data, Fig. S12). If we take into account EPR data, we find ~55±25% efficiency of TEMPO to TEMPOH conversion. The unambiguous determination of the chemical shifts of terephthalic acid (8.07 ppm) and TEMPOH (CH₃, 1.33 and 1.37 ppm) was made on the basis of the additive method, i.e., measuring the ¹H NMR spectrum before and after adding a small amount of the studied substances. Insets to Figure S4 show the ¹H NMR spectra after addition of TEMPOH (right) and terephthalic acid (left).

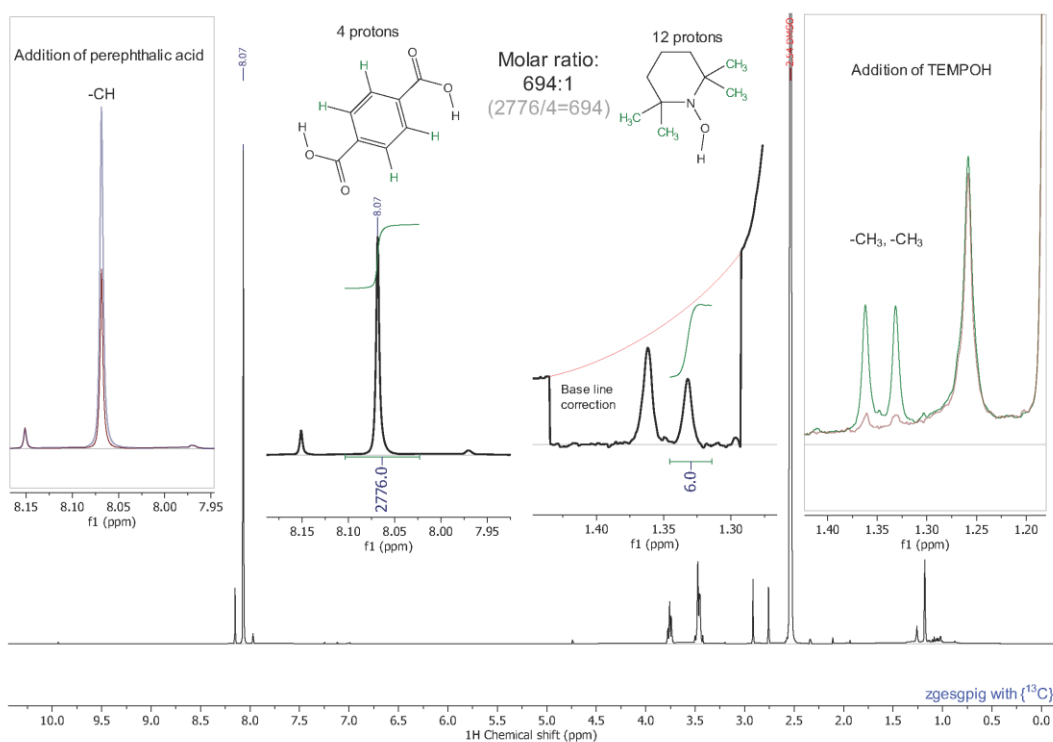


Fig. S4. 400 MHz ¹H{¹³C} NMR spectrum of TEMPOH@UiO-66 dissolved in HF/d₆-DMSO. NMR spectra before and after the addition of the studied substances (see insets) to the solution were measured to unambiguously determine the positions of the terephthalic acid and TEMPOH signals. Acquisition parameters: solvent suppression using excitation sculpting at 6.1 ppm, broadband ¹³C decoupling by garp4 composite pulses, number of scans 1024, repetition time 16s (at least three times longer than longest T₁-relaxation time). Before integration, the baseline correction I applied for region 1.3...1.45 ppm.

II.1. Supplementary EPR data

Kinetics of TEMPO@UiO-66 formation

To study the kinetics of nitroxide formation in the pores of UiO-66, the sample of TEMPOH·HCOOH@UiO-66 was first evacuated for 30 minutes at room temperature to remove the traces of acetonitrile. Then the sample was opened to air with simultaneous EPR control (Fig. S5). The nitroxide signal intensity grew gradually during about ~30 hours. We have found that the complete oxidation took 30-40 hours according to EPR spectroscopic data.

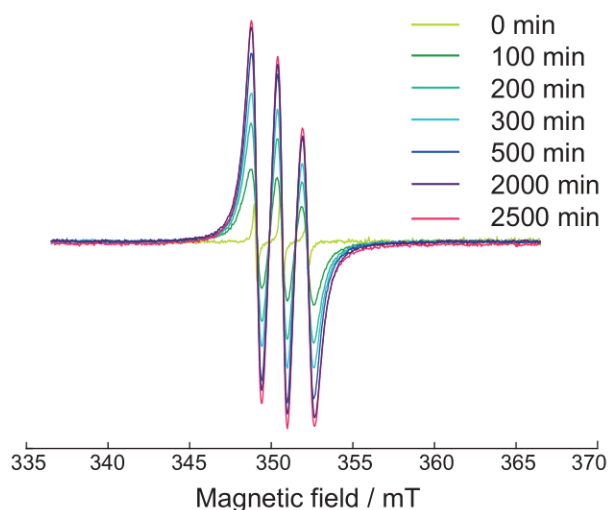


Fig. S5. X-band CW EPR spectra of TEMPO@UiO-66 vs. time. All spectra were measured at 298 K.

Methodology for characterization of the content of nitroxide probe in MOF pores

To estimate the TEMPO content in the pores of UiO-66 EPR, the following procedure was implemented. EPR spectra were recorded for the 50 μl TEMPO solution in toluene ($7 \cdot 10^{-5}$ M) and for the sample of TEMPO@UiO-66 (2 mg) with copper sulfate crystal hydrate as a reference (Fig. S6).

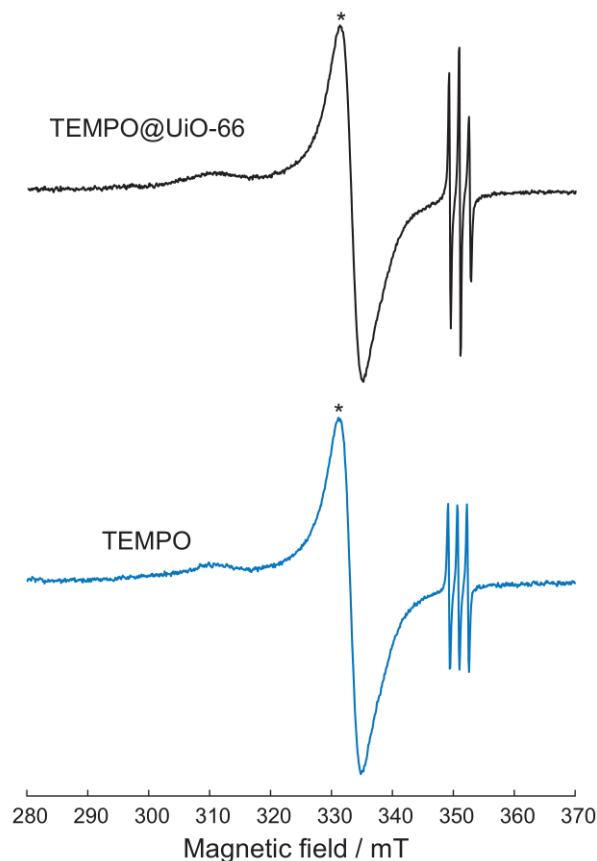


Fig. S6. X-band CW EPR spectra of TEMPO@UiO-66 (black curve) and TEMPO in toluene (blue curve). Spectra have been adjusted to a reference signal (*).

Reference sample was placed in a separate tube in the same resonator cavity. Spectra of TEMPO in toluene and TEMPO@UiO-66 were normalized to the signal of copper sulfate, which was the same in each experiment. Finally, amount of TEMPO in TEMPO@UiO-66 pores was calculated via comparison of second integrals of EPR spectra for TEMPO in toluene and TEMPO@UiO-66.

Encapsulation of TEMPO in UiO-66

To study nitroxide radical encapsulation inside the metal-organic framework we flushed the sample of TEMPO@UiO-66 with hexane 6 times (Fig. S7 (a)). As a control sample, we took the same TEMPO@UiO-66 and impregnated it with hexane without flushing (Fig. S7 (b)). For comparison, Figure S7 (c) also shows the spectrum of TEMPO dissolved in bulk hexane (0.5 mM solution).

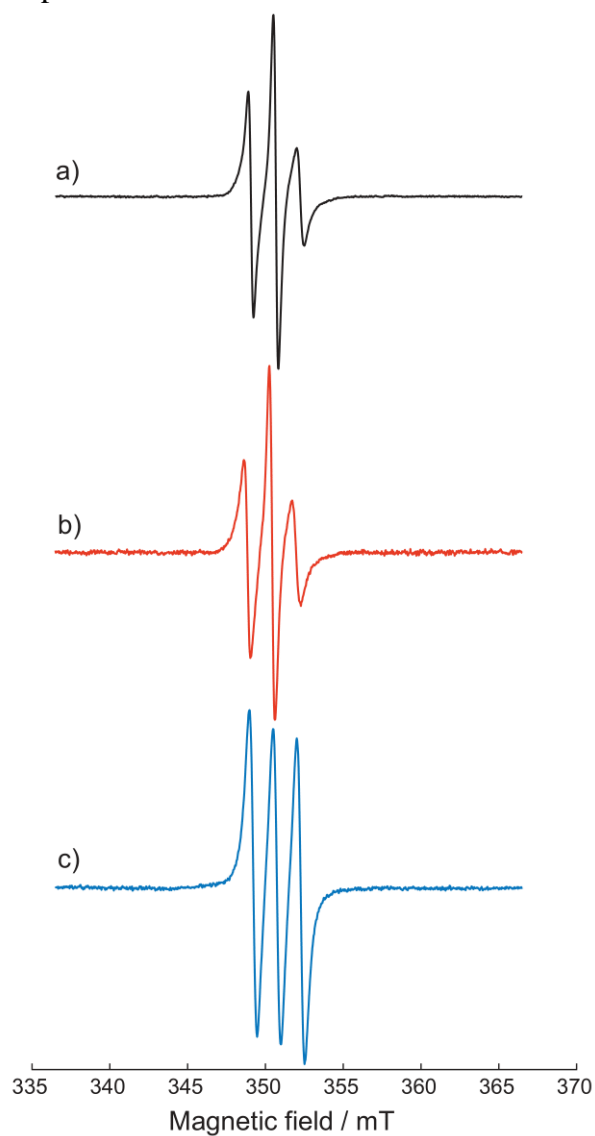


Fig. S7. X-band CW EPR spectra of TEMPO@UiO-66 in hexane with flushing (a) and without (b), TEMPO ($C = 5 \cdot 10^{-4}$ M) in hexane (c). All spectra have been adjusted to a reference signal.

Table S2. Parameters of X-band CW EPR spectra of TEMPO@UiO-66 shown in Fig. 3 and 4.

Sample	$[g_{xx} \ g_{yy} \ g_{zz}]$		$[A_{xx} \ A_{yy} \ A_{zz}] / \text{mT}$	τ_C / ns	λ_{20}	Linewidth / mT
evacuated	[2.0090 2.0085 2.0055]		[0.52 0.52 3.80]	1	0.3	[0 0.010]
air	[2.0090 2.0085 2.0055]		[0.52 0.52 3.80]	2.2	0.3	[0 0.155]
hexane	[2.0090 2.0085 2.0055]		[0.52 0.52 3.80]	1	0	[0 0.022]
after 0.13 GPa air	51%	[2.0090 2.0080 2.0040]	[0.62 0.62 3.50]	>100	0	[0 0.060]
	49%	[2.0090 2.0085 2.0055]	[0.52 0.52 3.80]	3.2	0.3	[0 0.060]
after 0.06 GPa	11%	[2.0090 2.0080 2.0040]	[0.62 0.62 3.50]	>100	0	[0 0.060]
	89%	[2.0090 2.0085 2.0055]	[0.52 0.52 3.80]	2.2	0.3	[0 0.155]

It should be noted that the EPR spectra with hexane are significantly different compared to the spectrum of TEMPO dissolved in hexane (Fig. S7 (c)); thus, it can be concluded that the nitroxide cannot leave the pores of UiO-66 and remains permanently entrapped (encapsulated) there.

Mechanical pressure applied to TEMPO@ZIF-8

For comparison with UiO-66, we also studied the effect of low mechanical pressure on another MOF, ZIF-8, with encapsulated TEMPO radicals. For this purpose, TEMPO@ZIF-8 was compressed using ~ 0.13 GPa for 10 minutes with a hydraulic press.

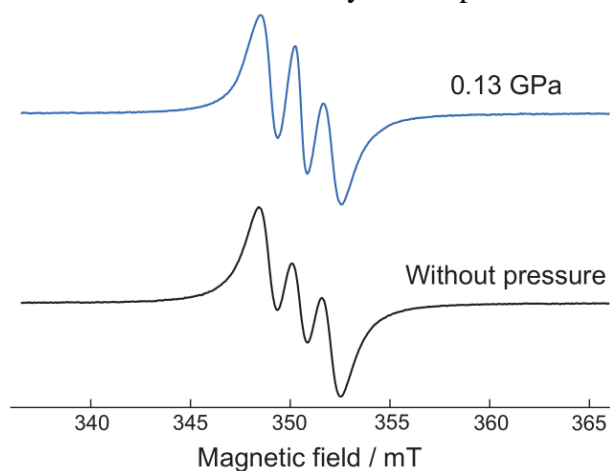


Fig. S8. X-band CW EPR spectra of activated TEMPO@ZIF-8: without pressure (black curve) and after external pressure of 0.13 GPa within 10 minutes (blue curve). Spectra were measured at 298 K and all spectra are normalized.

No significant changes in the EPR spectrum of the sample were observed after its exposure to external pressure (Fig. S8), whereas amorphization of ZIF-8 leads to the drastic changes in nitroxide EPR spectra.^{S2}

Different mechanical pressure applied to TEMPO@UiO-66

To investigate the effect of pressure on TEMPO@UiO-66 in more detail, we applied pressures from 0.13 to 1.17 GPa to the TEMPO@UiO-66 samples (Fig. S9). EPR spectra are quite similar, and an increase in pressure does not lead to any noticeable evolution of the system. This may be due to the fact that at low pressure (0.13 GPa) the porous system has already been fully collapsed.

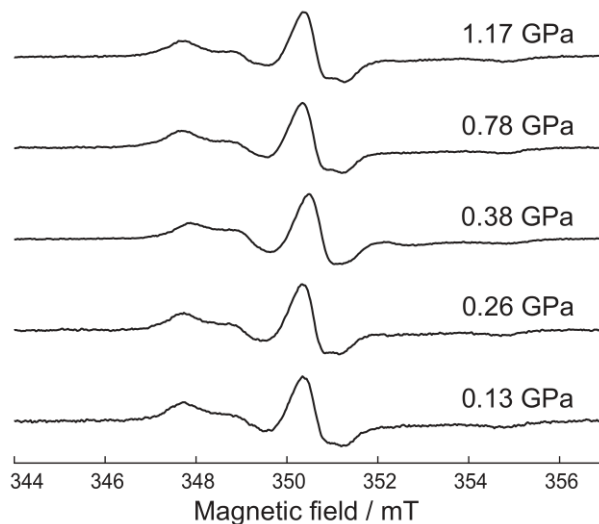


Fig. S9. X-band CW EPR spectra of TEMPO@UiO-66 after different external pressures of 0.13, 0.26, 0.38, 0.78 and 1.17 GPa. Spectra were measured at 298 K.

To study how time of pressure exposure affects the extent of destruction in TEMPO@UiO-66, we measured EPR spectra after different pressurization time: 5, 10 and 30 min (Fig. S10). It is clear that the porous system has collapsed within first 5 minutes.

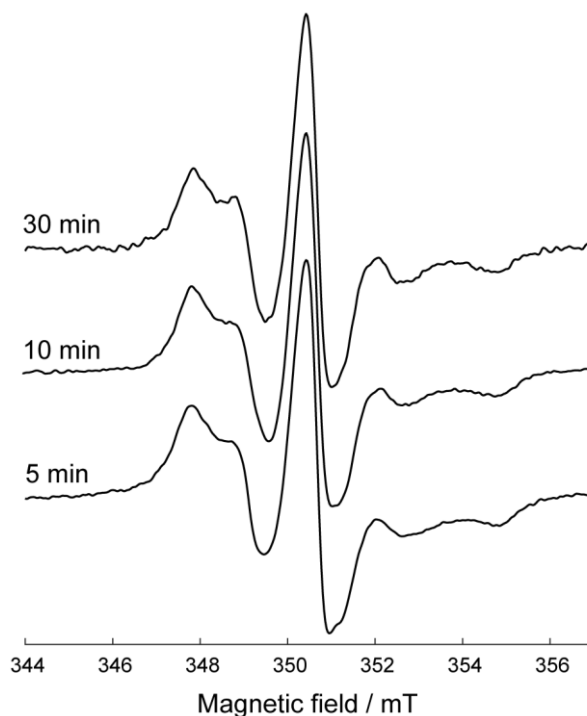


Fig. S10. X-band CW EPR spectra of TEMPO@UiO-66 after different pressurization time at 0.13 GPa.

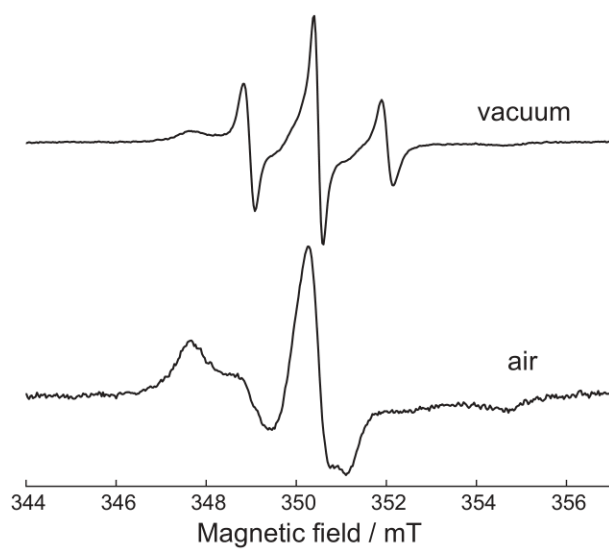


Fig. S11. X-band CW EPR spectra of TEMPO@UiO-66 after external pressures of 0.13 GPa (below) and the same sample under evacuation (above).

II.2. Supplementary TGA data

The amount of defects was established by TGA analysis using the established method.^{S3}

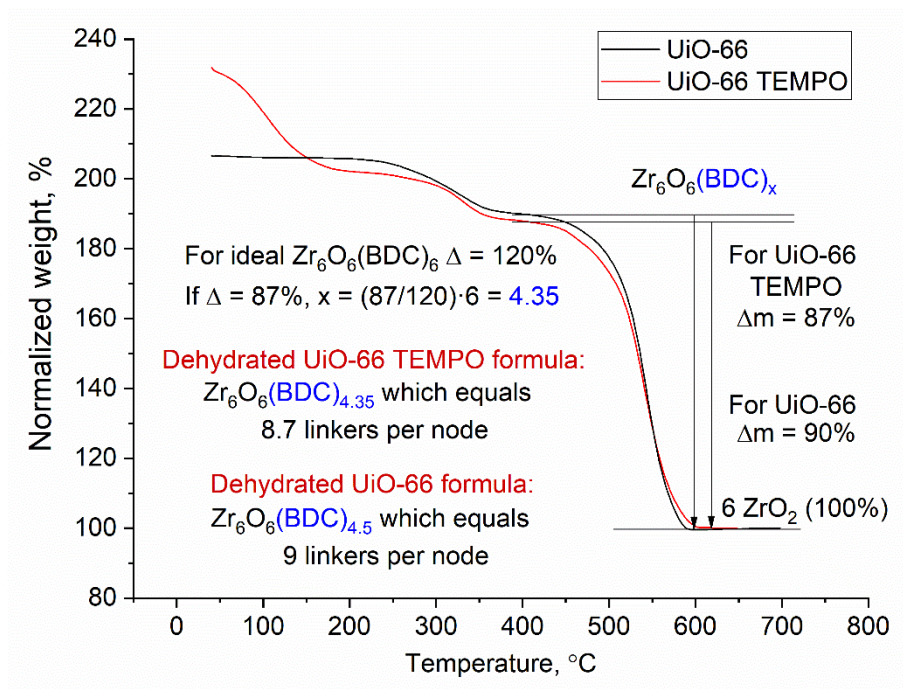


Fig. S12. TGA curve for UiO-66 (black) and TEMPO@UiO-66 (red).

II.3. Supplementary PXRD data

To investigate how external pressure affects the crystallinity of TEMPO@UiO-66 we used PXRD. The sample has been placed under pressure of 0.13 GPa for 10 minutes. The PXRD pattern was collected when the pressure was released. The characteristic peaks of metal-organic framework UiO-66 are still clearly visible (Fig. S13 (a)), however there is some contribution of the amorphous phase (Fig. S13 (b)) in the form of a baseline blur, indicating the onset of amorphization process.

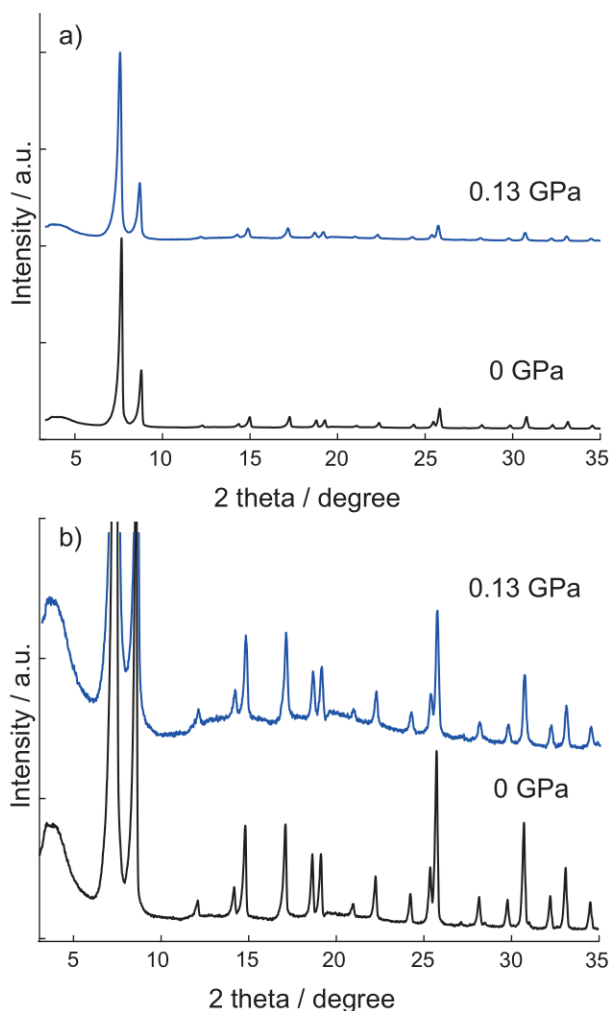


Fig. S13. PXRD data for TEMPO@UiO-66 (black) without any external pressure and TEMPO@UiO-66 after 10 minutes under 0.13 GPa (blue), (*) peak is corresponded to aluminium sample holder.

According to the PXRD data, we can conclude that the sample does not lose its crystallinity completely, but only undergoes partial amorphization at relatively low pressure.

II.4. Supplementary N₂ adsorption measurements

The nitrogen gas adsorption isotherm at 77 K for UiO-66 after exposure to external pressure 0.13 GPa showed a negligible decrease in nitrogen uptake (1032 m²/g) compared to its initial sample (1113 m²/g); moreover, no change in the isotherm patterns was observed (Fig. S14).

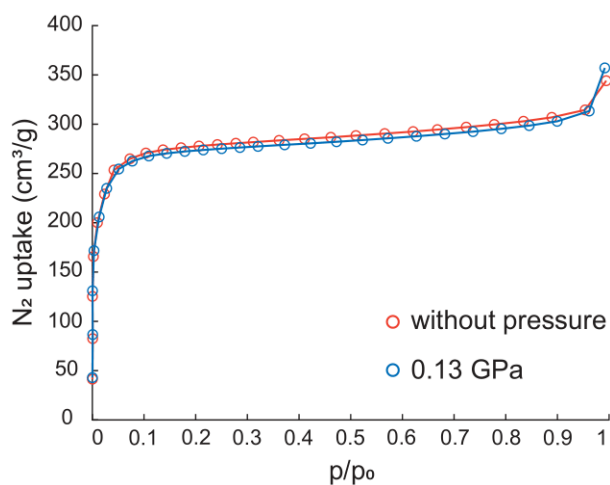


Fig. S14. N₂ adsorption isotherms for UiO-66: without pressure (red) and after external pressure of 0.13 GPa within 10 minutes (blue) at 77 K.

Table S3. BET surface area of different samples UiO-66.

Compound	UiO-66	UiO-66 after 0.13 GPa	TEMPO@UiO-66
BET surface area (m ² /g)	1113	1032	1073

III. References

- (S1) Cavka, J. H.; Jakobsen, S.; Olsbye, U.; Guillou, N.; Lamberti, C.; Bordiga, S.; Lillerud, K. P. A New Zirconium Inorganic Building Brick Forming Metal Organic Frameworks with Exceptional Stability. *J. Am. Chem. Soc.* **2008**, *130* (42), 13850–13851. <https://doi.org/10.1021/ja8057953>
- (S2) Poryvaev, A. S.; Polyukhov, D. M.; Fedin, M. V. Mitigation of Pressure-Induced Amorphization in Metal-Organic Framework ZIF-8 upon EPR Control. *ACS Appl. Mater. Interfaces* **2020**, *12* (14), 16655–16661. <https://doi.org/10.1021/acsami.0c03462>
- (S3) Valenzano, L.; Civalleri, B.; Chavan, S.; Bordiga, S.; Nilsen, M. H.; Jakobsen, S.; Lillerud, K. P.; Lamberti, C. Disclosing the complex structure of UiO-66 metal organic framework: a synergic combination of experiment and theory. *Chemistry of Materials* **2011**, *23*(7), 1700-1718. <https://doi.org/10.1021/cm1022882>